

Pre-defined Time Sliding Mode Control for Nonlinear Systems Based on Neural Networks

Wenhui Zhang, Rui Chen, Changliang Xu, Hua Liu

Abstract—For the problem of predefined-time control of nonlinear systems with unknown elements, a predefined-time non-singular terminal sliding mode control based on affective neural networks is proposed. Initially, a predefined-time sliding mode controller is designed using sliding mode control and predefined-time stability theory. Subsequently, unknown components in the nonlinear system are approximated using affective neural networks, and the introduction of a saturation function addresses the singularity issue inherent in traditional terminal sliding mode control. This is integrated with an equivalent controller to design a new controller. Finally, the proposed control methodology is thoroughly analyzed for stability using Lyapunov's stability theorem, and its effectiveness is validated through simulation examples.

Index Terms—Predefined time control, Nonsingular control, Terminal sliding mode control, Nonlinear system, Neural network control

I. INTRODUCTION

In the field of control, the theory of nonlinear systems control has been continuously evolving and improving. Although most studies have focused on the asymptotic stability or boundedness of the systems, in practical engineering applications, control objectives are often expected to be achieved within a limited timeframe [1]-[2]. Thus, precisely controlling a system to reach synchronization within a predefined period holds significant value. Compared to traditional non-finite time stability methods, finite-time stability has become particularly important in practical control systems where strict convergence time requirements are necessary due to its higher convergence precision and faster convergence speed. Although finite-time control strategies ensure that the system's state convergence time is bounded, the actual convergence time is limited by the system's initial state. This results in significant variability in convergence difficult to accurately predict the exact convergence time.

Manuscript received December 23, 2024; revised March 24, 2025.

This work was supported by the National Natural Science Foundation of China (61772247), the Industry-Academia-Research Cooperation Projects of Jiangsu Province (BY2022651), the Key Foundation projects of Lishui (2023LTH03), Zhejiang Qianlin Sewing Equipment Co., Ltd. Doctoral Innovation Station, Discipline Construction Project of Lishui University (Discipline Fund Name: Mechanical Engineering).

Wenhui Zhang is a professor at Nanjing Xiaozhuang University, Nanjing 211171, P. R. China (e-mail: hit_zwh@126.com).

Rui Chen is a postgraduate student in the School of Mechanical Engineering at Zhejiang Sci-Tech University, Hangzhou 310018, P. R. China (corresponding author to provide phone: +86-18265787665; email: cr1716707642@126.com).

Changliang Xu is a lecturer at Nanjing Xiaozhuang University, Nanjing 211171, P. R. China (e-mail: xcl987765@126.com).

Hua Liu is a lecturer at Nanjing Xiaozhuang University, Nanjing 211171, P. R. China (e-mail: 10962655@126.com).

To address the dependency of finite-time stability on initial states, fixed-time stability has been proposed. Unlike finite-time stability, fixed-time stability is independent of the system's initial conditions, ensuring stability within a predetermined fixed time for any initial state, with an upper bound on the convergence time that can be calculated through parameters [3]-[4].

Although the convergence time for fixed-time stability is determinable, the complex relationship between control parameters and stabilization time often leads to overly conservative estimates of convergence time. To address this issue, predefined-time control was proposed. This strategy allows for the adjustment of predefined time parameters, thereby enhancing the certainty and stability of system convergence times. Reference [5] introduced a novel predefined-time neural learning control strategy aimed at synchronizing chaotic systems with unknown dynamics. This approach integrates control laws and parameter update rules, consistent with predefined-time Lyapunov theory, to ensure that synchronization errors converge rapidly and precisely to a minimal value near zero. The effectiveness of this method was validated through simulations, highlighting its robustness and adaptability in managing chaotic systems. In addressing the control issues of multi-joint uncertain robots, input saturation effects often adversely impact system performance. To tackle this challenge, Reference [6] proposed an adaptive and practical predefined-time neural tracking control strategy. This approach is based on predefined-time stability design and employs radial basis function neural networks (RBFNN) to approximate the unknown dynamics of robot manipulators. By dynamically compensating for input saturation, this strategy ensures that tracking errors converge to a small neighborhood near the origin within a predefined time, irrespective of initial conditions. Numerical simulations and experimental results have demonstrated that this control strategy significantly enhances precision and responsiveness in robotic arms with up to nine joints, outperforming traditional methods. In response to the challenge of predefined-time smooth control under external disturbances, Reference [7] introduced a neural adaptive control method. This approach utilizes adaptive neural networks to predict and compensate for unknown nonlinearities and disturbances in robot manipulator arms, ensuring that the system states converge accurately to the desired trajectory within the set time. By avoiding singularity issues and dynamically adjusting control parameters to adapt to external changes, the strategy significantly enhanced the system's overall robustness. Reference [8] addressed the synchronization issue of

uncertain hyperchaotic systems and introduced a novel predefined-time sliding mode control (SMC) approach. This strategy involves a new sliding mode function and its corresponding controller that ensure errors in synchronization converge effectively to the sliding surface within a predefined time. The method excels in managing uncertainties, external disturbances, and time delays within the system, significantly enhancing the system's robustness and dynamic performance. Reference [9] proposed a novel adjustable predefined-time non-singular terminal sliding mode control (TSMC) method. This method innovatively combined adjustable predefined-time stability (PTS), radial basis function neural networks, and the robustness of sliding mode control. It effectively resolved the issues of singularity and unknown model dynamics that were present in traditional terminal sliding mode control methods. In addressing the control challenges of strict-feedback nonlinear systems, Reference [10] introduced a new adaptive command-filtered predefined-time fuzzy control approach. This method employed fuzzy logic systems to estimate uncertain functions within the control system, and integrated command filters to tackle the issue of "complexity explosion" commonly encountered in controller design. To effectively manage the errors introduced by command filtering, an improved command filter compensation mechanism was proposed, thereby enhancing the overall stability and response speed of the system.

Based on the analysis and discussions above, this study developed a novel predefined-time non-singular terminal sliding mode control based on affective neural networks. The main innovations include:

(1) A new control strategy was designed based on the proposed predefined-time stability lemma, ensuring that the system achieves predefined-time stability during both the sliding and reaching phases.

(2) The study introduced a method incorporating saturation functions, which not only overcame the issue of singularity but also ensured the system reached the predefined-time stability.

(3) A new controller based on the emotion neural network (ENN) was developed, addressing the challenge of unknown model information and ensuring that the system stably reached the sliding surface within the set time. Additionally, a complete proof of predefined-time stability based on the Lyapunov method was provided.

I. PROBLEM STATEMENT

A. Key Definitions and Lemmas

Consider a class of nonlinear systems:

$$\dot{x} = f(x), \quad f(0) = 0 \tag{1}$$

Here, $x \in \mathbb{R}^m$ represent the state vector of the system, and $f(x)$ is a nonlinear continuous function.

Lemma 1: [11] For system 1, there exists a Lyapunov function that satisfies the following conditions:

$$\dot{V}(x) \leq -\frac{\pi}{\sqrt{\alpha\beta\eta T_c}} \left(\alpha(V(x))^{1-\frac{\eta}{2}} + \beta(V(x))^{1+\frac{\eta}{2}} \right) + \Omega \tag{2}$$

Here, $\alpha > 0, \beta > 0, 0 < \eta < 1, T_c > 0$, and $0 < \Omega < +\infty$.

Then, system 1 can actually achieve predefined-time stability, stabilizing in the vicinity of the origin:

$$\lim_{t \rightarrow T} x | V(x) \leq \min \left\{ \left(\frac{\eta T_c \sqrt{\alpha\beta\Omega}}{\pi\alpha(1-\tau)} \right)^{1-\frac{\eta}{2}}, \left(\frac{\eta T_c \sqrt{\alpha\beta\Omega}}{\pi\beta(1-\tau)} \right)^{1+\frac{\eta}{2}} \right\} \tag{3}$$

Here, $\tau \in (0,1)$, within a bounded settling time $T \leq T_c / \sqrt{\tau}$.

Lemma 2: [12] If x_1, x_2, \dots, x_n is a positive scalar and $0 < c < 1, d > 1$, then it follows that:

$$\left(\sum_{i=1}^n |x_i|^c \right) \leq \sum_{i=1}^n |x_i|^c$$

$$n^{1-d} \left(\sum_{i=1}^n |x_i|^d \right) \leq \sum_{i=1}^n |x_i|^d \tag{4}$$

B. Problem Formulation

A single-input single-output second-order nonlinear system can be described as follows:

$$\begin{cases} \dot{x}_1 = x_2 \\ \dot{x}_2 = f(x) + g(x)u(t) + \psi(x,t) \\ y = x \end{cases} \tag{5}$$

Here, $x = [x_1, x_2]^T$ represents the state vector, $f(x)$ is an unknown nonlinear function, $g(x)$ is a known smooth nonlinear function, $u(t)$ is the control input, $\psi(x,t)$ is the external disturbance, and y is the system output.

Assumption 1: The system's uncertainties and disturbances are bounded, and there exists a known constant $\ell > 0$ such that $|\psi(x,t)| < \ell$ [13]-[14].

According to equation (5), the tracking error:

$$e_1 = x_1 - x_{1d} \tag{6}$$

Here, x_{1d} is the expected value of x_1 .

II. PREDEFINED-TIME NON-SINGULAR SLIDING MODE CONTROL

To ensure that the variable e_1 converges within the predetermined time during the sliding phase, The sliding surface is as follows:

$$s = \dot{e}_1 + \left(\frac{1}{2} \right)^{1-\frac{\eta}{2}} \frac{\pi\alpha^{\frac{1}{2}}\beta^{\frac{1}{2}}}{\eta_1 T_1} |e_1|^{1-\eta} \text{sign}(e_1)$$

$$+ \left(\frac{1}{2} \right)^{1+\frac{\eta}{2}} \frac{\pi\alpha^{\frac{1}{2}}\beta^{\frac{1}{2}}}{\eta_1 T_1} |e_1|^{1+\eta} \text{sign}(e_1) \tag{7}$$

Here, $\eta \in (0,1), T_1 > 0, \alpha > 0, \beta > 0$.

Take the derivative of s

$$\dot{s} = \ddot{e}_1 + \left(\frac{1}{2} \right)^{1-\frac{\eta}{2}} (1-\eta_1) \frac{\pi\alpha^{\frac{1}{2}}\beta^{\frac{1}{2}}}{\eta_1 T_1} \dot{e}_1 e_1^{-\eta}$$

$$+ \left(\frac{1}{2} \right)^{1+\frac{\eta}{2}} (1+\eta_1) \frac{\pi\alpha^{\frac{1}{2}}\beta^{\frac{1}{2}}}{\eta_1 T_1} \dot{e}_1 e_1^{\eta} \tag{8}$$

By integrating equations (5) and (6) into equation (8), the equivalent controller is obtained as follows:

$$u_{eq} = \frac{1}{g(x)} \left[\ddot{x}_d - f(x) - \left(\frac{1}{2}\right)^{1-\frac{\eta_1}{2}} (1-\eta_1) \frac{\pi\alpha^{\frac{1}{2}}\beta^{-\frac{1}{2}}}{\eta_1 T_1} \dot{e}_1 e_1^{-\eta_1} - \left(\frac{1}{2}\right)^{1+\frac{\eta_1}{2}} (1+\eta_1) \frac{\pi\alpha^{\frac{1}{2}}\beta^{\frac{1}{2}}}{\eta_1 T_1} \dot{e}_1 e_1^{\eta_1} \right] \quad (9)$$

From equation (9), it is evident that the presence of $\dot{e}_1 e_1^{-\eta_1}$ in the equivalent controller introduces a singularity issue when $e_1 = 0, e_2 \neq 0$. Therefore, a saturation function is incorporated into the controller to address this singularity problem. The saturation function is defined as follows:

$$sat(x) = \begin{cases} x & x \leq h \\ hsign(x) & x > h \end{cases} \quad (10)$$

Then the equivalent controller can be written as:

$$u_{x_{eq}} = \frac{1}{g(x)} \left[\ddot{x}_d - f(x) - sat \left[\left(\frac{1}{2}\right)^{1-\frac{\eta_1}{2}} (1-\eta_1) \frac{\pi\alpha^{\frac{1}{2}}\beta^{-\frac{1}{2}}}{\eta_1 T_1} \dot{e}_1 e_1^{-\eta_1} - \left(\frac{1}{2}\right)^{1+\frac{\eta_1}{2}} (1+\eta_1) \frac{\pi\alpha^{\frac{1}{2}}\beta^{\frac{1}{2}}}{\eta_1 T_1} \dot{e}_1 e_1^{\eta_1} \right] \right] \quad (11)$$

In the controller, to approximate unknown terms, an ENN is employed. The ENN comprises four main parts: the hypothalamus, sensory cortex, amygdala, and orbitofrontal cortex (OFC) [15]. Within the hypothalamus layer, each node corresponds to a radial basis function, constructed as follows:

$$g_i = \exp \left(-\frac{(\delta - \gamma_i)^T (\delta - \gamma_i)}{b_i^2} \right), i = 1, 2, 3, \dots, j$$

Here, $\delta = [\delta_1, \delta_2, \delta_3, \dots, \delta_n]^T$ represents the input vector to the ENN, γ_i denotes the mean, j is the number of nodes in the hypothalamus, and b_i is the standard deviation.

The sensory cortex primarily functions as a distributor, relaying the vector of radial basis functions to the amygdala and the OFC. The outputs from the amygdala and OFC are as follows:

$$E_a = \sum_{i=1}^j V_i g_i = V^T g \quad (13)$$

$$E_o = \sum_{i=1}^j W_i g_i = W^T g \quad (14)$$

The total output of ENN is:

$$E = E_a - E_o = (V - W)^T g \quad (15)$$

Here, $V = [V_1, V_2, \dots, V_j]$ represents the weights of the amygdala, and $W = [W_1, W_2, \dots, W_j]$ denotes the weights of the OFC.

The unknown term $f(x)$ is approximated using the ENN, expressed as follows:

$$f(x) = (V^* - W^*)^T g^* + \varepsilon \quad (16)$$

$$g^* = g^*(\delta, \gamma^* b^*) \quad (17)$$

Here, V^*, W^* represents the optimal weights, ε denotes

the minimum error, γ^* is the optimal mean error, and b^* indicates the optimal standard deviation.

$$\hat{f}(x) = (\hat{V} - \hat{W})^T \hat{g} \quad (18)$$

$$\begin{aligned} \Lambda &= (V^* - W^*)^T g^* - (\hat{V} - \hat{W})^T \hat{g} + \varepsilon \\ &= (V^* - W^*)^T (\hat{g} + \tilde{g}) - (\hat{V} - \hat{W})^T \hat{g} + \varepsilon \\ &= [(\hat{V} - \hat{W})^T + (\tilde{V} - \tilde{W})^T] (\hat{g} + \tilde{g}) - (\hat{V} - \hat{W})^T \hat{g} + \varepsilon \\ &= (\hat{V} - \hat{W})^T \tilde{g} + (\tilde{V} - \tilde{W})^T \tilde{g} + \varepsilon + (\tilde{V} - \tilde{W})^T \hat{g} \\ &= (\tilde{V} - \tilde{W})^T \hat{g} + (\hat{V} - \hat{W})^T \tilde{g} + \varepsilon_r \end{aligned} \quad (19)$$

Here, $\hat{V}, \hat{W}, \hat{g}$ are the estimated values of V^*, W^*, g^* , $V^* - \hat{V} = \tilde{V}$, $W^* - \hat{W} = \tilde{W}$, $g^* - \hat{g} = \tilde{g}$, $\varepsilon_r = (\tilde{V} - \tilde{W})^T \tilde{g} + \varepsilon$.

The nonlinear activation function is converted to a partially linear form by Taylor expansion, Perform a Taylor expansion of \tilde{g} at the point $g^* = g^*(\delta, \gamma^* b^*)$ [16].

$$Dg_\gamma = \left[\frac{\partial \hat{g}}{\partial \gamma_1}, \dots, \frac{\partial \hat{g}}{\partial \gamma_m}, \dots, \frac{\partial \hat{g}}{\partial \gamma_j} \right]^T \Bigg|_{\gamma=\hat{\gamma}} \in R^{j \times j} \quad (20)$$

$$Dg_b = \left[\frac{\partial \hat{g}}{\partial b_1}, \dots, \frac{\partial \hat{g}}{\partial b_m}, \dots, \frac{\partial \hat{g}}{\partial b_j} \right]^T \Bigg|_{b=\hat{b}} \in R^{j \times j} \quad (21)$$

$$\begin{aligned} \tilde{g} &= \frac{\partial g}{\partial \gamma} \Bigg|_{\gamma=\hat{\gamma}} (\gamma^* - \hat{\gamma}) + \frac{\partial g}{\partial b} \Bigg|_{b=\hat{b}} (b^* - \hat{b}) + O_h \\ &= Dg_\gamma \tilde{\gamma} + Dg_b \tilde{b} + O_h \end{aligned} \quad (22)$$

Here, O_h represents the higher-order terms. Substituting equations (20)-(22) into equation (19), yields the following:

$$\Lambda = (\tilde{V} - \tilde{W})^T \hat{g} + (\hat{V} - \hat{W})^T (Dg_\gamma \tilde{\gamma} + Dg_b \tilde{b} + O_h) + \varepsilon_r \quad (23)$$

The overall system controller is as follows:

$$\begin{aligned} u &= u_{x_{eq}} + u_{sw} = \frac{1}{g(x)} \left[\ddot{x}_d - (\hat{V} - \hat{W})^T \hat{g} - sat \left[\left(\frac{1}{2}\right)^{1-\frac{\eta_1}{2}} (1-\eta_1) \frac{\pi\alpha^{\frac{1}{2}}\beta^{-\frac{1}{2}}}{\eta_1 T_1} \dot{e}_1 e_1^{-\eta_1} - \left(\frac{1}{2}\right)^{1+\frac{\eta_1}{2}} (1+\eta_1) \frac{\pi\alpha^{\frac{1}{2}}\beta^{\frac{1}{2}}}{\eta_1 T_1} \dot{e}_1 e_1^{\eta_1} + \left[-\left(\frac{1}{2}\right)^{1-\frac{\eta_2}{2}} \frac{\pi\alpha^{\frac{1}{2}}\beta^{-\frac{1}{2}}}{\eta_2 T_2} |s|^{1-\eta_2} sign(s) - \left(\frac{1}{2}\right)^{1+\frac{\eta_2}{2}} \frac{\pi\alpha^{\frac{1}{2}}\beta^{\frac{1}{2}}}{\eta_2 T_2} |s|^{1+\eta_2} sign(s) - Ksign(s) \right] \right] \right] \quad (24) \end{aligned}$$

$$\begin{aligned} u_{sw} &= \frac{1}{g(x)} \left[-\left(\frac{1}{2}\right)^{1-\frac{\eta_2}{2}} \frac{\pi\alpha^{\frac{1}{2}}\beta^{-\frac{1}{2}}}{\eta_2 T_2} |s|^{1-\eta_2} sign(s) - \left(\frac{1}{2}\right)^{1+\frac{\eta_2}{2}} \frac{\pi\alpha^{\frac{1}{2}}\beta^{\frac{1}{2}}}{\eta_2 T_2} |s|^{1+\eta_2} sign(s) - Ksign(s) \right] \quad (25) \end{aligned}$$

Here, $0 < \eta_2 < 1, T_2$ is a positive constant.

III. STABILITY ANALYSIS

$$M = \left\{ (e_1, \dot{e}_1) : \left[\begin{pmatrix} 1 \\ 2 \end{pmatrix}^{1-\frac{\eta}{2}} (1-\eta) \frac{\pi\alpha^{\frac{1}{2}}\beta^{\frac{1}{2}}}{\eta T_1} \dot{e}_1 e_1^{-\eta} \right] \leq \varpi \right\}$$

$$N = \left\{ (e_1, \dot{e}_1) : \left[\begin{pmatrix} 1 \\ 2 \end{pmatrix}^{1-\frac{\eta}{2}} (1-\eta) \frac{\pi\alpha^{\frac{1}{2}}\beta^{\frac{1}{2}}}{\eta T_1} \dot{e}_1 e_1^{-\eta} \right] > \varpi \right\} \quad (27)$$

Lemma 3: Given the existing second-order nonlinear system, along with the designed sliding surface and controller, and employing the neural network proposed in this paper, the sliding variable and error converge within a predefined time. According to the lemma 1, the convergence time satisfies $T_c \leq T_1 + T_2/\sqrt{\tau}$, $\tau \in (0,1)$ [17]-[20].

Construct the Lyapunov function as follows:

$$V_1 = \frac{1}{2}s^2 + B \quad (28)$$

Here, $B = \frac{1}{2\lambda_1} tr(\tilde{V}^T \tilde{V}) + \frac{1}{2\lambda_2} tr(\tilde{W}^T \tilde{W}) + \frac{1}{2\lambda_3} tr(\tilde{\gamma}^T \tilde{\gamma}) + \frac{1}{2\lambda_4} tr(\tilde{b}^T \tilde{b})$. The learning parameter $\lambda_1, \lambda_2, \lambda_3, \lambda_4$ is adjusted to the optimal solution based on the adaptation rate.

Differentiating equation (28) yields:

$$\dot{V}_1 = s\dot{s} + \dot{B} \quad (29)$$

Substituting equations (6) and (8) into equation (29) results in:

$$\begin{aligned} \dot{V}_1 &= s\dot{s} + \dot{B} \\ &= s\left(\ddot{e}_1 + \left(\frac{1}{2}\right)^{1-\frac{\eta}{2}} (1-\eta) \frac{\pi\alpha^{\frac{1}{2}}\beta^{\frac{1}{2}}}{\eta T_1} \dot{e}_1 e_1^{-\eta}\right) \\ &\quad + \left(\frac{1}{2}\right)^{1+\frac{\eta}{2}} (1+\eta) \frac{\pi\alpha^{\frac{1}{2}}\beta^{\frac{1}{2}}}{\eta T_1} \dot{e}_1 e_1^{\eta} + \dot{B} \\ &= s(\ddot{x}_1 - \ddot{x}_d + \left(\frac{1}{2}\right)^{1-\frac{\eta}{2}} (1-\eta) \frac{\pi\alpha^{\frac{1}{2}}\beta^{\frac{1}{2}}}{\eta T_1} \dot{e}_1 e_1^{-\eta}) \\ &\quad + \left(\frac{1}{2}\right)^{1+\frac{\eta}{2}} (1+\eta) \frac{\pi\alpha^{\frac{1}{2}}\beta^{\frac{1}{2}}}{\eta T_1} \dot{e}_1 e_1^{\eta} + \dot{B} \\ &= s(f(x) + g(x)u(t) + \psi(x,t) - \ddot{x}_d) \\ &\quad + \left(\frac{1}{2}\right)^{1-\frac{\eta}{2}} (1-\eta) \frac{\pi\alpha^{\frac{1}{2}}\beta^{\frac{1}{2}}}{\eta T_1} \dot{e}_1 e_1^{-\eta} \\ &\quad + \left(\frac{1}{2}\right)^{1+\frac{\eta}{2}} (1+\eta) \frac{\pi\alpha^{\frac{1}{2}}\beta^{\frac{1}{2}}}{\eta T_1} \dot{e}_1 e_1^{\eta} + \dot{B} \end{aligned} \quad (30)$$

Substituting the overall controller (24) into equation (30) yields:

$$\begin{aligned} \dot{V}_1 &= s(f(x) + g(x)u(t) + \psi(x,t) - \ddot{x}_d) \\ &\quad + \left(\frac{1}{2}\right)^{1-\frac{\eta}{2}} (1-\eta) \frac{\pi\alpha^{\frac{1}{2}}\beta^{\frac{1}{2}}}{\eta T_1} \dot{e}_1 e_1^{-\eta} \end{aligned}$$

$$\begin{aligned} &+ \left(\frac{1}{2}\right)^{1+\frac{\eta}{2}} (1+\eta) \frac{\pi\alpha^{\frac{1}{2}}\beta^{\frac{1}{2}}}{\eta T_1} \dot{e}_1 e_1^{\eta} + \dot{B} \\ &= s \left[f(x) + g(x) \left[\frac{1}{g(x)} \left[\ddot{x}_d - (\hat{V} - \hat{W})^T \hat{g} \right. \right. \right. \\ &\quad \left. \left. \left. - sat \left[\left(\frac{1}{2}\right)^{1-\frac{\eta}{2}} (1-\eta) \frac{\pi\alpha^{\frac{1}{2}}\beta^{\frac{1}{2}}}{\eta T_1} \dot{e}_1 e_1^{-\eta} \right] \right. \right. \right. \\ &\quad \left. \left. \left. - \left(\frac{1}{2}\right)^{1+\frac{\eta}{2}} (1+\eta) \frac{\pi\alpha^{\frac{1}{2}}\beta^{\frac{1}{2}}}{\eta T_1} \dot{e}_1 e_1^{\eta} \right. \right. \right. \\ &\quad \left. \left. \left. + \left[-\left(\frac{1}{2}\right)^{1-\frac{\eta}{2}} \frac{\pi\alpha^{\frac{1}{2}}\beta^{\frac{1}{2}}}{\eta_2 T_2} |s|^{1-\eta_2} sign(s) \right. \right. \right. \\ &\quad \left. \left. \left. - \left(\frac{1}{2}\right)^{1+\frac{\eta}{2}} \frac{\pi\alpha^{\frac{1}{2}}\beta^{\frac{1}{2}}}{\eta_2 T_2} |s|^{1+\eta_2} sign(s) - Ksign(s) \right] \right] \right] \\ &\quad + \psi(x,t) - \ddot{x}_d + \left(\frac{1}{2}\right)^{1-\frac{\eta}{2}} (1-\eta) \frac{\pi\alpha^{\frac{1}{2}}\beta^{\frac{1}{2}}}{\eta T_1} \dot{e}_1 e_1^{-\eta} \\ &\quad + \left(\frac{1}{2}\right)^{1+\frac{\eta}{2}} (1+\eta) \frac{\pi\alpha^{\frac{1}{2}}\beta^{\frac{1}{2}}}{\eta T_1} \dot{e}_1 e_1^{\eta} + \dot{B} \end{aligned} \quad (31)$$

When (e_1, \dot{e}_1) is within the range of M , it can be obtained as follows:

$$\begin{aligned} &sat \left[\left(\frac{1}{2}\right)^{1-\frac{\eta}{2}} (1-\eta) \frac{\pi\alpha^{\frac{1}{2}}\beta^{\frac{1}{2}}}{\eta T_1} \dot{e}_1 e_1^{-\eta} \right] \\ &= \left(\frac{1}{2}\right)^{1-\frac{\eta}{2}} (1-\eta) \frac{\pi\alpha^{\frac{1}{2}}\beta^{\frac{1}{2}}}{\eta T_1} \dot{e}_1 e_1^{-\eta} \end{aligned} \quad (32)$$

Thus, rearranging equation 31 yields:

$$\begin{aligned} \dot{V}_1 &= s \left[(\tilde{V} - \tilde{W})^T \hat{g} + (\hat{V} - \hat{W})^T (D\mathcal{G}_\gamma \tilde{\gamma} + D\mathcal{G}_b \tilde{b} + O_h) \right. \\ &\quad \left. + \varepsilon_\tau - \left(\frac{1}{2}\right)^{1-\frac{\eta}{2}} \frac{\pi\alpha^{\frac{1}{2}}\beta^{\frac{1}{2}}}{\eta_2 T_2} |s|^{1-\eta_2} sign(s) \right. \\ &\quad \left. - \left(\frac{1}{2}\right)^{1+\frac{\eta}{2}} \frac{\pi\alpha^{\frac{1}{2}}\beta^{\frac{1}{2}}}{\eta_2 T_2} |s|^{1+\eta_2} sign(s) - Ksign(s) + \psi(x,t) \right] + \dot{B} \\ &= s \left[(\tilde{V} - \tilde{W})^T \hat{g} + (\hat{V} - \hat{W})^T (D\mathcal{G}_\gamma \tilde{\gamma} + D\mathcal{G}_b \tilde{b} + O_h) \right. \\ &\quad \left. + \varepsilon_\tau - \left(\frac{1}{2}\right)^{1-\frac{\eta}{2}} \frac{\pi\alpha^{\frac{1}{2}}\beta^{\frac{1}{2}}}{\eta_2 T_2} |s|^{1-\eta_2} sign(s) \right. \\ &\quad \left. - \left(\frac{1}{2}\right)^{1+\frac{\eta}{2}} \frac{\pi\alpha^{\frac{1}{2}}\beta^{\frac{1}{2}}}{\eta_2 T_2} |s|^{1+\eta_2} sign(s) - Ksign(s) + \psi(x,t) \right] \\ &\quad + \frac{1}{\lambda_1} tr(-\tilde{V}^T \dot{\tilde{V}}) + \frac{1}{\lambda_2} tr(-\tilde{W}^T \dot{\tilde{W}}) + \frac{1}{\lambda_3} tr(-\tilde{\gamma}^T \dot{\tilde{\gamma}}) + \frac{1}{\lambda_4} tr(-\tilde{b}^T \dot{\tilde{b}}) \\ &= s\tilde{V}^T \hat{g} - s\tilde{W}^T \hat{g} + s(\hat{V} - \hat{W})^T D\mathcal{G}_\gamma \tilde{\gamma} + s(\hat{V} - \hat{W})^T D\mathcal{G}_b \tilde{b} + \end{aligned}$$

$$\begin{aligned}
 & s \left[(\hat{V} - \hat{W})^T O_h + \varepsilon_\tau - \left(\frac{1}{2}\right)^{1-\frac{\eta_2}{2}} \frac{\pi\alpha^{\frac{1}{2}}\beta^{\frac{1}{2}}}{\eta_2 T_2} |s|^{1-\eta_2} \text{sign}(s) \right. \\
 & \left. - \left(\frac{1}{2}\right)^{1+\frac{\eta_2}{2}} \frac{\pi\alpha^{\frac{1}{2}}\beta^{\frac{1}{2}}}{\eta_2 T_2} |s|^{1+\eta_2} \text{sign}(s) - K \text{sign}(s) + \psi(x, t) \right] \\
 & + \frac{1}{\lambda_1} \text{tr}(-\tilde{V}^T \dot{\hat{V}}) + \frac{1}{\lambda_2} \text{tr}(-\tilde{W}^T \dot{\hat{W}}) + \frac{1}{\lambda_3} \text{tr}(-\tilde{\gamma}^T \dot{\hat{\gamma}}) \\
 & + \frac{1}{\lambda_4} \text{tr}(-\tilde{b}^T \dot{\hat{b}}) \tag{33}
 \end{aligned}$$

Set the adaptation rate as follows:

$$\dot{\hat{V}} = \lambda_1 \hat{g} \max(s, 0) \tag{34}$$

$$\dot{\hat{W}} = \lambda_2 \hat{g} s \tag{35}$$

$$\dot{\hat{\gamma}}^T = \lambda_3 (\hat{V} - \hat{W}) s D \mathcal{G}_\gamma \tag{36}$$

$$\dot{\hat{b}}^T = \lambda_4 (\hat{V} - \hat{W}) s D \mathcal{G}_b \tag{37}$$

Organize the relevant terms to obtain:

$$\begin{aligned}
 \dot{V}_1 &= \tilde{V}^T \hat{g} (s - \max(s, 0)) \\
 & + s \left[\varepsilon_0 - \left(\frac{1}{2}\right)^{1-\frac{\eta_2}{2}} \frac{\pi\alpha^{\frac{1}{2}}\beta^{\frac{1}{2}}}{\eta_2 T_2} |s|^{1-\eta_2} \text{sign}(s) \right. \\
 & \left. - \left(\frac{1}{2}\right)^{1+\frac{\eta_2}{2}} \frac{\pi\alpha^{\frac{1}{2}}\beta^{\frac{1}{2}}}{\eta_2 T_2} |s|^{1+\eta_2} \text{sign}(s) - K \text{sign}(s) \right] \tag{38}
 \end{aligned}$$

Here, $\varepsilon_0 = (\hat{V} - \hat{W})^T O_h + \varepsilon_\tau + \psi(x, t)$, $s - \max(s, 0) \leq s$, assuming $|\tilde{V}^T \hat{g} + \varepsilon_0| \leq \mathbb{Z}$, equation (38) is rewritten as:

$$\dot{V}_1 = |s| (\mathbb{Z} - K) \tag{39}$$

When $K > \mathbb{Z}$, it can be obtained as follows:

$$\dot{V}_1 \leq 0 \tag{40}$$

Thus, the method proposed ensures the stability of the system. An analysis of the predefined time will now be conducted.

Based on lemma 2 and Lyapunov function (28), equation (38) can be derived as follows:

$$\begin{aligned}
 \dot{V}_1 &\leq s \left[-\left(\frac{1}{2}\right)^{1-\frac{\eta_2}{2}} \frac{\pi\alpha^{\frac{1}{2}}\beta^{\frac{1}{2}}}{\eta_2 T_2} |s|^{1-\eta_2} \text{sign}(s) \right. \\
 & \left. - \left(\frac{1}{2}\right)^{1+\frac{\eta_2}{2}} \frac{\pi\alpha^{\frac{1}{2}}\beta^{\frac{1}{2}}}{\eta_2 T_2} |s|^{1+\eta_2} \text{sign}(s) \right] \\
 &\leq -\left(\frac{1}{2}\right)^{1-\frac{\eta_2}{2}} \frac{\pi\alpha^{\frac{1}{2}}\beta^{\frac{1}{2}}}{\eta_2 T_2} |s|^{2-\eta_2} - \left(\frac{1}{2}\right)^{1+\frac{\eta_2}{2}} \frac{\pi\alpha^{\frac{1}{2}}\beta^{\frac{1}{2}}}{\eta_2 T_2} |s|^{2+\eta_2} \\
 &\leq -\frac{\pi\alpha^{\frac{1}{2}}\beta^{\frac{1}{2}}}{\eta_2 T_2} \left(\frac{1}{2} s^2\right)^{1-\frac{\eta_2}{2}} - \frac{\pi\alpha^{\frac{1}{2}}\beta^{\frac{1}{2}}}{\eta_2 T_2} \left(\frac{1}{2} s^2\right)^{1+\frac{\eta_2}{2}} \\
 &\leq -\frac{\pi\alpha^{\frac{1}{2}}\beta^{\frac{1}{2}}}{\eta_2 T_2} \left[\left(\frac{1}{2} s^2\right)^{1-\frac{\eta_2}{2}} - B^{1-\frac{\eta_2}{2}} + B^{1+\frac{\eta_2}{2}} \right]
 \end{aligned}$$

$$\begin{aligned}
 & -\frac{\pi\alpha^{\frac{1}{2}}\beta^{\frac{1}{2}}}{\eta_2 T_2} \left[\left(\frac{1}{2} s^2\right)^{1+\frac{\eta_2}{2}} - B^{1+\frac{\eta_2}{2}} + B^{1-\frac{\eta_2}{2}} \right] \\
 & \leq -\frac{\pi\alpha^{\frac{1}{2}}\beta^{\frac{1}{2}}}{\eta_2 T_2} \left[\left(\frac{1}{2} s^2 + B\right)^{1-\frac{\eta_2}{2}} - B^{1-\frac{\eta_2}{2}} \right] \\
 & \quad -\frac{\pi\alpha^{\frac{1}{2}}\beta^{\frac{1}{2}}}{\eta_2 T_2} \left[\left(\frac{1}{2} s^2 + B\right)^{1+\frac{\eta_2}{2}} - B^{1+\frac{\eta_2}{2}} \right] \\
 & \leq -\frac{\pi\alpha^{\frac{1}{2}}\beta^{\frac{1}{2}}}{\eta_2 T_2} \left[\left(\frac{1}{2} s^2 + B\right)^{1-\frac{\eta_2}{2}} \right] + \frac{\pi\alpha^{\frac{1}{2}}\beta^{\frac{1}{2}}}{\eta_2 T_2} B^{1-\frac{\eta_2}{2}} \\
 & \quad -\frac{\pi\alpha^{\frac{1}{2}}\beta^{\frac{1}{2}}}{\eta_2 T_2} \left[\left(\frac{1}{2} s^2 + B\right)^{1+\frac{\eta_2}{2}} \right] + \frac{\pi\alpha^{\frac{1}{2}}\beta^{\frac{1}{2}}}{\eta_2 T_2} B^{1+\frac{\eta_2}{2}} \\
 & \leq -\frac{\pi}{\sqrt{\alpha\beta}\eta_2 T_2} \left[\alpha(V_1)^{1-\frac{\eta_2}{2}} + \beta(V_1)^{1+\frac{\eta_2}{2}} \right] \\
 & \quad + \frac{\pi\alpha^{\frac{1}{2}}\beta^{\frac{1}{2}}}{\eta_2 T_2} B^{1-\frac{\eta_2}{2}} + \frac{\pi\alpha^{\frac{1}{2}}\beta^{\frac{1}{2}}}{\eta_2 T_2} B^{1+\frac{\eta_2}{2}} \\
 & \leq -\frac{\pi}{\sqrt{\alpha\beta}\eta_2 T_2} \left[\alpha(V_1)^{1-\frac{\eta_2}{2}} + \beta(V_1)^{1+\frac{\eta_2}{2}} \right] + \Omega \tag{41}
 \end{aligned}$$

According to lemma 1, the designed closed-loop system can stabilize within a predefined time.

$$\lim_{t \rightarrow T} x |V_1(x) \leq \min \left\{ \left(\frac{\eta T_2 \sqrt{\alpha\beta}\Omega}{\pi\alpha(1-\tau)} \right)^{1-\frac{\eta}{2}}, \left(\frac{\eta T_2 \sqrt{\alpha\beta}\Omega}{\pi\beta(1-\tau)} \right)^{1+\frac{\eta}{2}} \right\} \tag{42}$$

Here, $\tau \in (0, 1)$, At the predefined time $T \leq T_2 / \sqrt{\tau}$,

$$\Omega = \frac{\pi\alpha^{\frac{1}{2}}\beta^{\frac{1}{2}}}{\eta_2 T_2} B^{1-\frac{\eta_2}{2}} + \frac{\pi\alpha^{\frac{1}{2}}\beta^{\frac{1}{2}}}{\eta_2 T_2} B^{1+\frac{\eta_2}{2}}, \Omega \text{ is widely used in}$$

the existing literature. Since Ω is a function related to the adaptive law of the ENN and its approximation properties are broadly similar to those of the RBFNN, it follows that Ω is bounded.

When (e_1, \dot{e}_1) are within the range of N , it can be concluded that:

$$e_1(t) = e_1(0) + \int_0^t \dot{e}_1(\theta) d\theta \tag{43}$$

When $\dot{e}_1 > 0$, $e_1(t)$ is monotonically increasing, and when $\dot{e}_1 < 0$, $e_1(t)$ is monotonically decreasing. According to reference [21], (e_1, \dot{e}_1) will leave region M and will not permanently stay within this region. The existence of region N does not affect the stability analysis, and the introduced saturation function does not interfere with the performance of the controller, as the proportion of time passing through region N during the convergence process is very small.

In summary, the sliding variable converges to the zero domain within the predefined time $T_2 / \sqrt{\tau}$.

Lemma 4: When the terminal sliding mode surface s

converges near the zero point, the tracking error will converge to the origin within the predefined time T_1 [22]-[26].

When $s = 0$, it can be deduced that:

$$\begin{aligned} \dot{e}_1 = & -\left(\frac{1}{2}\right)^{1-\frac{\eta_1}{2}} \frac{\pi\alpha^{\frac{1}{2}}\beta^{-\frac{1}{2}}}{\eta_1 T_1} |e_1|^{1-\eta_1} \text{sign}(e_1) \\ & -\left(\frac{1}{2}\right)^{1+\frac{\eta_1}{2}} \frac{\pi\alpha^{-\frac{1}{2}}\beta^{\frac{1}{2}}}{\eta_1 T_1} |e_1|^{1+\eta_1} \text{sign}(e_1) \end{aligned} \quad (44)$$

Define the Lyapunov function as:

$$V_2 = \frac{1}{2} e_1^2 \quad (45)$$

Differentiating Equation (45) yields:

$$\begin{aligned} \dot{V}_2 = & \frac{1}{2} \dot{e}_1^2 \\ = & e_1 \dot{e}_1 \\ = & e_1 \left[-\left(\frac{1}{2}\right)^{1-\frac{\eta_1}{2}} \frac{\pi\alpha^{\frac{1}{2}}\beta^{-\frac{1}{2}}}{\eta_1 T_1} |e_1|^{1-\eta_1} \text{sign}(e_1) \right. \\ & \left. -\left(\frac{1}{2}\right)^{1+\frac{\eta_1}{2}} \frac{\pi\alpha^{-\frac{1}{2}}\beta^{\frac{1}{2}}}{\eta_1 T_1} |e_1|^{1+\eta_1} \text{sign}(e_1) \right] \\ = & -\left(\frac{1}{2}\right)^{1-\frac{\eta_1}{2}} \frac{\pi\alpha^{\frac{1}{2}}\beta^{-\frac{1}{2}}}{\eta_1 T_1} |e_1|^{2-\eta_1} - \left(\frac{1}{2}\right)^{1+\frac{\eta_1}{2}} \frac{\pi\alpha^{-\frac{1}{2}}\beta^{\frac{1}{2}}}{\eta_1 T_1} |e_1|^{2+\eta_1} \\ = & -\frac{\pi}{\sqrt{\alpha\beta}\eta_1 T_1} \left(\alpha(V_2)^{1-\frac{\eta_1}{2}} + \beta(V_2)^{1+\frac{\eta_1}{2}} \right) \end{aligned} \quad (46)$$

Based on the aforementioned theorem, the tracking error converges within the predefined time T_1 . The proof concludes here.

IV. SIMULATION AND DISCUSSION

A simulation analysis using a single-joint robotic arm was conducted to validate the effectiveness of the proposed method[27]-[32]. The dynamics of the system are as follows:

$$\begin{cases} \dot{x}_1 = x_2 \\ \dot{x}_2 = -\frac{1}{I}(dx_2 + mgl \cos x_1) + \frac{1}{I}u - \frac{1}{I}\psi_d \end{cases} \quad (47)$$

Here, In the system, $x_1 = \theta$ represents the output angle,

$x_2 = \dot{\theta}$ the angular velocity, $I = \frac{1}{3}ml^2$ the moment of

inertia of the robotic arm, with an arm length of $l = 0.3$, a viscous friction coefficient of $d = 2$, a mass of $m = 1.5$, and the gravitational constant $g = 10$.

The specific form of the unknown nonlinear friction model ψ_d is as follows:

$$\psi_d = \sigma(x_2)F_c(x_2) + [1 - \sigma(x_2)]F_s(x_2) \quad (48)$$

$$\sigma(x_2) = \begin{cases} 1, & |x_2| \geq D_e \\ 0, & |x_2| < D_e \end{cases} \quad (49)$$

Here, The coulomb friction upper limit is $\bar{F}_c = 0.6$, the

static friction upper limit is $\bar{F}_s = 1.0$, $D_e = 0.025$, $F_c(x_2) = 0.6 \exp(-3.5|x_2| \text{sign}(x_2))$, $F_s(x_2) = 1.0 \text{sign}(x_2)$, the desired trajectory is set as $x_d = \sin(\pi t/3)$, and the initial state of the system is $x_1 = \frac{\pi}{6}$, $x_2 = 0$. Controller parameters are selected as $T_1 = T_2 = 0.5$ and $\eta_1 = \eta_2 = 0.2$.

To validate the advantages of the control method proposed in this paper, it was compared with a fixed-time control method. The parameters involved in the comparative method were determined by empirical and trial-and-error methods.

The fixed-time control in the literature utilizes equations (50) and (51) [33]-[35]:

$$s = \dot{e}_1 + \xi_1 |e_1|^{\lambda_1} \text{sign}(e_1) + \xi_2 |e_1|^{\lambda_2} \text{sign}(e_1) \quad (50)$$

$$\begin{aligned} u = & -g(x)[f(x) - x_{1d} + \text{sat}(\xi_1 \lambda_1 |e_1|^{\lambda_1 - 1} \dot{e}_1) \\ & + \xi_2 \lambda_2 |e_1|^{\lambda_2 - 1} \dot{e}_1 + \xi_3 |s|^{\lambda_3} \text{sign}(s) \\ & + \xi_4 |s|^{\lambda_4} \text{sign}(s) + D_2 \text{sign}(s)] \end{aligned} \quad (51)$$

$$\text{Here, } \lambda_1 = \frac{z_1 + 1}{2} + \frac{1 - z_1}{2} \text{sign}(|e_1| - 1), \quad 0 < z_1,$$

$$\lambda_2 = \frac{z_2 + 1}{2} + \frac{1 - z_2}{2} \text{sign}(|e_1| - 1), \quad 1 < z_2,$$

$$\lambda_3 = \frac{v_1 + 1}{2} + \frac{1 - v_1}{2} \text{sign}(|s| - 1), \quad v_1, \quad v_2 > 1,$$

$$\lambda_4 = \frac{v_2 + 1}{2} + \frac{1 - v_2}{2} \text{sign}(|s| - 1), \quad \xi_1, \quad \xi_2, \quad \xi_3, \quad \xi_4 > 0,$$

$$D_2 > 0.$$

The simulation results are as follows:

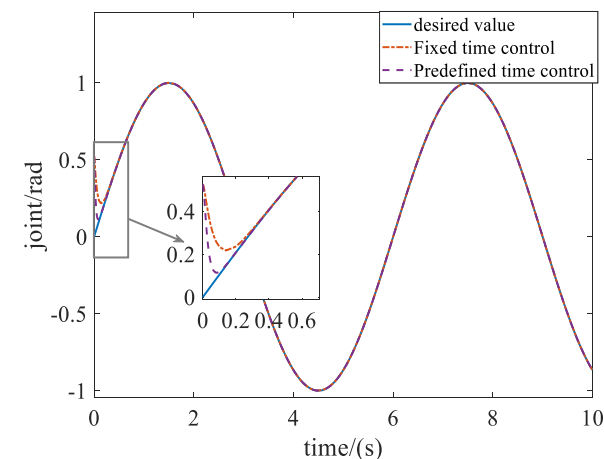


Fig. 1. Position trajectory tracking curves

Fig. 1 shows the angle trajectory tracking of a single robotic arm, and Fig. 2 presents the tracking error. From the figures, it is observed that the designed predefined-time control achieves good tracking of the desired value around 0.2s, while the fixed-time control stabilizes the error after about 0.42s. This demonstrates that the predefined-time error converges faster and in a shorter time compared to fixed-time error, resulting in better tracking performance of the desired values.

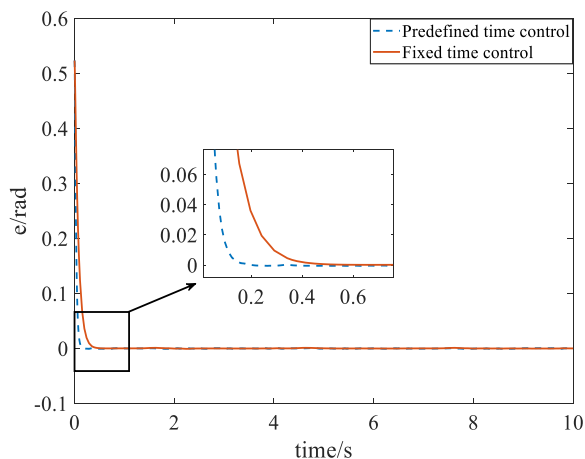


Fig. 2. Tracking error curve

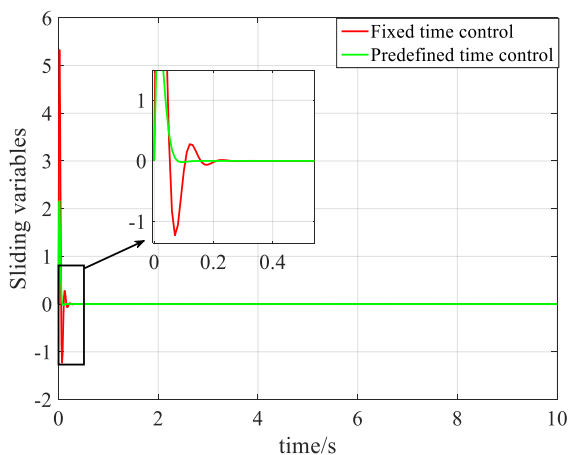


Fig. 3. sliding surface curves

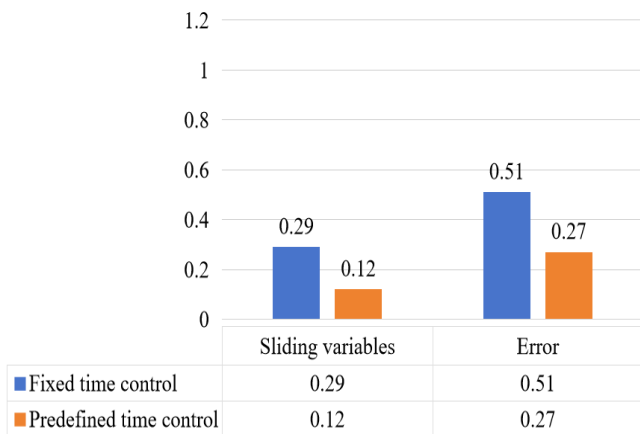


Fig. 4. Convergence time

Fig. 3 shows that both control schemes exhibit relatively good control performance under steady-state conditions. However, when comparing the stabilization time and process, the designed predefined-time control converges to a sliding variable of zero faster and with less fluctuation. Fig. 4 displays the convergence time of the sliding mode variable and the actual performance of the tracking error under different control strategies. The actual convergence times all fall within the preset convergence time range, and this preset convergence time is not influenced by the controller parameters, making it more adaptable to the needs of actual control engineering.

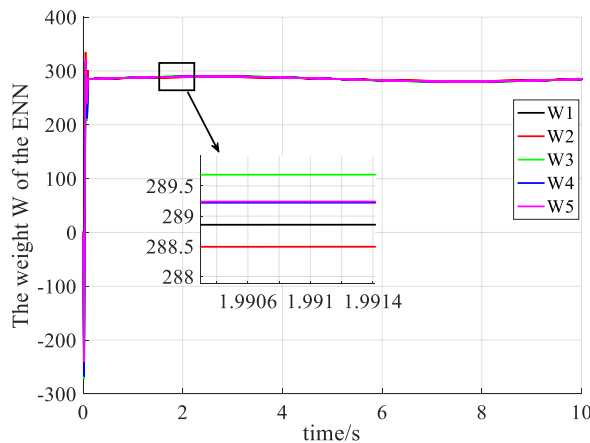


Fig. 5. The weights of the OFC

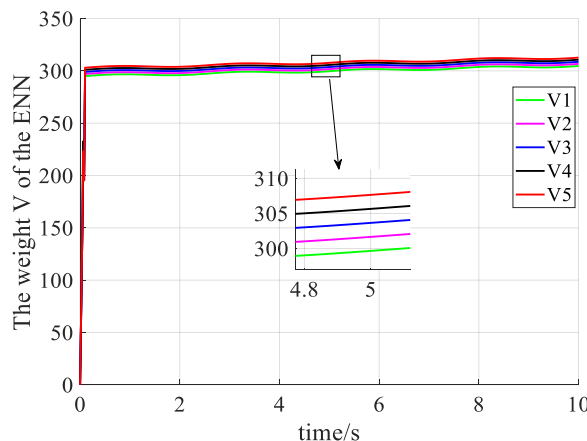


Fig. 6. The weights of the amygdala

Fig. 5 and Fig. 6 illustrate the changes in the weights of the amygdala and OFC in the proposed ENN. Fig. 5 shows fluctuations in the weight W of the OFC after it trends towards stability. Fig. 6 depicts the weight V of the amygdala, which continues to exhibit a slow increasing trend after becoming relatively stable. These observations confirm that the proposed controller aligns with the characteristics of the ENN.

V. CONCLUSIONS

A predefined-time non-singular terminal sliding mode control based on an ENN was proposed, ensuring that the tracking error is predefined-time stable during both the reaching and sliding phases. The ENN approximates unknown elements in the system model and utilizes a saturation function to address the singularity issues of terminal sliding mode. Finally, experimental simulations demonstrated that the proposed control method offers superior control performance and stability compared to other control methods.

REFERENCES

- [1] J. Shen, W. Zhang, S. Zhou, et al. "Fuzzy Adaptive Compensation Control for Space Manipulator with Joint Flexibility and Dead Zone Based on Neural Network," *International Journal of Aeronautical and Space Sciences*, vol.24, no.3, pp. 876-889, 2023.
- [2] Li-Jian Jiang, Wen-Hui Zhang, Jin-Miao Shen, Yang-Fan Ye, and Shu-Hua Zhou, "Vibration Suppression of Flexible Joints Space Robot based on Neural Network," *IAENG International Journal of Applied Mathematics*, vol.52, no.4, pp776-783, 2022

- [3] W. Zhang, J. Shen, X. Ye, et al. "Error model-oriented vibration suppression control of free-floating space robot with flexible joints based on adaptive neural network," *Engineering Applications of Artificial Intelligence*, vol.114, no.4, 105028, 2022.
- [4] Y. Hu, W. Zhang, "Modeling framework for analyzing midair encounters in hybrid airspace where manned and unmanned aircraft coexist. Proceedings of the Institution of Mechanical Engineers," Part G: Journal of Aerospace Engineering, vol.233, no.15, pp. 5492-5506, 2019.
- [5] Q. Yao, Q. Li, A. Alotaibi, et al. "Neural Learning Control Methodology for Predefined-Time Synchronization Of Unknown Chaotic Systems," *Fractals*, vol.31, no.06, pp. 2340146, 2023.
- [6] H. Sai, Z. Xu, E. Zhang, "Adaptive practical predefined-time neural tracking control for multi-joint uncertain robotic manipulators with input saturation," *Neural Computing and Applications*, vol.35, no.27, pp. 20423-20440, 2023.
- [7] Y. Fan, C. Yang, H. Zhan, et al. "Neuro-Adaptive-Based Predefined-Time Smooth Control for Manipulators with Disturbance," *IEEE Transactions on Systems, Man, and Cybernetics: Systems*, 2024.
- [8] W. Zheng, S. Qu, Q. Tang, "Predefined-time synchronization for uncertain hyperchaotic system with time-delay via sliding mode control," *Nonlinear Dynamics*, vol.112, no.24, pp. 21969-21987, 2024.
- [9] C. Jia, X. Liu, "Tunable predefined time nonsingular terminal sliding mode control based on neural network for nonlinear systems," *IEEE Access*, 2023.
- [10] Y. Jiang, Y. Su, "Adaptive Command Filtered Predefined-Time Fuzzy Control of Nonlinear Systems," 2024 43rd Chinese Control Conference (CCC), vol.112, IEEE, pp. 381-386, 2024.
- [11] C. Wu, J. Yan, J. Shen, et al. "Predefined-time attitude stabilization of receiver aircraft in aerial refueling," *IEEE Transactions on Circuits and Systems II: Express Briefs*, vol.68, no.10, pp. 3321-3325, 2021.
- [12] L. Cui, N. Jin, S. Chang, et al. "Fixed-time ESO based fixed-time integral terminal sliding mode controller design for a missile," *ISA transactions*, vol.125, pp. 237-251, 2022.
- [13] X. Guo, W. Zhang, and F. Z. Gao, "Global Prescribed-Time Stabilization of Input-Quantized Nonlinear Systems via State-Scale Transformation," *Electronics*, vol.12, no.15, pp. 1-18, 2023.
- [14] W. Zhang, H. S. Liu, X. P. Ye, et al. "Adaptive robust control for free-floating space robot Adaptive robust control for free-floating space robot with unknown uncertainty based on neural network with unknown uncertainty based on neural network," *International Journal of Advanced Robotic Systems*, vol.15, no.6, pp. 1-11, 2018.
- [15] J. Morén, C. Balkenius, "A computational model of emotional learning in the amygdala," *From animals to animats*, vol.6, pp. 115-124, 2000.
- [16] Jin-Miao Shen, Wen-Hui Zhang, Shu-Hua Zhou, and Xiao-Ping Ye, "Vibration Suppression Control of Space Flexible Manipulator with Varying Load Based on Adaptive Neural Network," *IAENG International Journal of Computer Science*, vol.50, no.2, pp.449-458, 2023
- [17] W. Zhang, F. Z. Gao, J. C. Huang, et al. "Global Prescribed-Time Stabilization for a Class of Uncertain Feedforward Nonlinear Systems," *IEEE Transactions on Circuits and Systems II: Express Briefs*, vol.70, no.4, pp. 1450-1454, 2022.
- [18] W. Zhang, X. P. Ye, L. H. Jiang, et al. "Output feedback control for free-floating space robotic manipulators base on adaptive fuzzy neural network," *Aerospace Science and Technology*, vol.29, no.1, pp. 135-143, 2013.
- [19] D. J. Sánchez-Torres, D. Gómez-Gutiérrez, E. López, et al. "A class of predefined-time stable dynamical systems," *IMA Journal of Mathematical Control and Information*, vol.35, Supplement_1, pp. i1-i29, 2018.
- [20] Wen-Hui Zhang, Yan-Ling Shang, Quan Sun, and Fang-Zheng Gao, "Finite-Time Stabilization of General Stochastic Nonlinear Systems with Application to a Liquid-Level System," *IAENG International Journal of Applied Mathematics*, vol.51, no. 2, pp.295-299, 2021
- [21] Y. Feng, X. Yu, F. Han, "On nonsingular terminal sliding-mode control of nonlinear systems," *Automatica*, vol.49, no. 6, pp. 1715-1722, 2013.
- [22] W. Zhang, N. Qi, J. Ma, et al. "Neural integrated control for free-floating space robot with changing parameters," *Science China: Information Science*, vol.54, pp. 2091-2099, 2011.
- [23] W. Zhang, X. Ye, X. Ji, et al. "RBF neural network adaptive control for space robots without speed feedback signal," *Transactions of the Japan Society for Aeronautical and Space Sciences*, vol.56, no.6, pp. 317-322, 2013.
- [24] Y. M. Fang, W. Zhang, and X. P. Ye, "Variable Structure Control for Space Robots Based on Neural Networks," *International Journal of Advanced Robotic Systems*, vol.11, no.3, pp. 35-42, 2014.
- [25] K. J. Ni, X. C. Liu, K. Liu, et al. "Finite-time sliding mode synchronization of chaotic systems," *Chinese Physics B*, vol.23, no.10, 100504, 2014.
- [26] W. Zhang, X. Ye, L. Jiang, and Y. Fang, "Robust Control of Robotic Manipulators Based on Adaptive Neural Network," *The Open Mechanical Engineering Journal*, Vol.8, No.1, pp. 497-502,2014.
- [27] X. C. Huang, Z. P. You, W. H. Zhang, et al, "Stabilization control of wheeled mobile robot based on neural sliding mode under wheel slip conditions," *International Journal of Dynamics and Control*, vol. 13, no.2, pp.1-12, 2025.
- [28] W. Zhang, Z. Wen, Y. Ye, and S. Zhou, "Structural mechanics analysis of bolt joint of rigid flexible coupling manipulator," *Journal of Measurements in Engineering*, vol.10, No.2, pp. 93-104,2022.
- [29] Da-Jian Yi, Zhang-Ping You, and Wen-Hui Zhang, "Image Enhancement CHPSO Processing Technology Based on Improved Particle Swarm Optimization Algorithm," *IAENG International Journal of Computer Science*, vol. 52, no.1, pp.130-142, 2025
- [30] W. Zhang, N. Qi, and Y. Li, "Output feedback PD control of robot manipulators dispense with model base on fuzzy-basis-function-network," *Journal of National University of Defense Technology*, vol.32, No.6, pp. 163-170,2010.
- [31] Zhang-Ping You, Da-Jian Yi, Zheng Fang, and Wen-Hui Zhang, "Image Enhancement ANPSO Processing Technology Based on Improved Particle Swarm Optimization Algorithm," *IAENG International Journal of Computer Science*, vol. 51, no.11, pp.1781-1792, 2024
- [32] W. Zhang, Y. Zhu, "Control of free-floating space robotic manipulators base on neural network," *International Journal of Computer Science Issues (IJCSI)*, vol.9, No.6, pp. 322, 2012.
- [33] J. Ma, W. Zhang, and H. P. Zhu, "Adaptive Control for Robotic Manipulators base on RBF Neural Network," *TELKOMNIKA*, vol.11, no.3, pp. 521-528, 2013.
- [34] L. Yin, W. Zhang, and T. Zhou, "Machine health-driven dynamic scheduling of hybrid jobs for flexible manufacturing shop," *International Journal of Precision Engineering and Manufacturing*, vol.24, no.5, pp.797-812, 2023.
- [35] W. Zhang, Y. Fang, X. Ye, "Adaptive Neural Network Robust Control for Space Robot with Uncertainty," *TELKOMNIKA*, vol.11, No.3, pp. 513-520, 2013.